

EXPERIMENTAL STUDY ON RC FRAMES WITH MASONRY INFILL CONSIDERING PARAMETERS INFLUENCING BACKBONE CURVE

Hamood ALWASHALI¹, Yuta TORIHATA², Kiwoong JIN³, Masaki MAEDA⁴

ABSTRACT

This paper presents test results of five $\frac{1}{2}$ scale single story reinforced concrete frames with masonry infill that were subjected to static cyclic lateral loading. Three main parameters were investigated: varying the strength of surrounding RC columns, varying the strength of RC beam and varying mortar strength of masonry infill. Those parameters were selected since there are significant variations between different design codes and past literature on the topic. Results showed that there is a great improvement in shear strength of infill with increasing the strength of surrounding frame. The post-peak degradation slope was also improved with increasing the ratio of frame shear strength to masonry infill. In addition, the investigated parameters did not significantly influence the initial stiffness even for specimen with weak mortar. The specimen with masonry infill of low strength mortar showed greater ductile behavior and relatively less damage in masonry infill panel and surrounding frame. Based on the results of this study, the seismic capacity of masonry infill should not be calculated based solely on the masonry material tests since surrounding frame can greatly change its seismic capacity. The parameter of ratio of frame strength to masonry infill should be taken into account in the design code of new RC buildings with masonry infill as it can totally change the seismic strength and ductility of masonry infill.

Keywords: Reinforced concrete; Masonry infill; Seismic capacity; Backbone curve

1. INTRODUCTION

Many RC buildings in the world use masonry infills as partition walls. The masonry infill is considered as a non-structural element but its influence on structural behavior has been repeatedly observed in recent earthquakes such as the 2009 L'Aquila earthquake in Italy, 2008 Sichuan earthquake in China, 1999 Izmit earthquake in Turkey, 2015 Nepal earthquake and the 2016 Ecuador earthquake. In general, masonry infill increases the frame strength, which is considered as a beneficial point. On the other hand, masonry infill exerts reaction forces on the RC frame causing additional moment and shear forces, which results in unexpected failure modes (FEMA 306 1998). In addition, the masonry infill greatly increases the frame stiffness that might change the seismic demand due to significant reduction in natural period of the building. Turgay et al. (2015) conducted a comparative study between different design codes that are used to estimate strength, deformation and stiffness of masonry infill. The comparative study showed large variation in the commonly used analytical models to calculate strength, deformation and stiffness. Another study by Al-Washali et al. (2017) showed also large variations between experimental results and equations proposed by various researchers, which tend to contradict each other or overly conservative. Due to these large variations between design codes in evaluating seismic capacity of masonry infill, many practicing engineers still assume that the walls are non-structural elements.

¹Ph.D. candidate, Graduate School of Engineering, Department of Architectural and Building Science, Tohoku University, Sendai, Japan Hamood@rcl.archi.tohoku.ac.jp

²Graduate student, Graduate School of Engineering, Department of Architectural and Building Science, Tohoku University, Sendai, Japan Torihata@rcl.archi.tohoku.ac.jp

³Assistant professor, Graduate School of Engineering, Department of Architectural and Building Science, Tohoku University, Sendai, Japan Jin@rcl.archi.tohoku.ac.jp

⁴Professor, Graduate School of Engineering, Department of Architectural and Building Science, Tohoku University, Sendai, Japan Maeda@rcl.archi.tohoku.ac.jp

The large variations of different codes are resulted from incomplete knowledge of masonry infill material and parameters affecting its seismic performance. Therefore, the objective of this study is to clarifying the impact of several major parameters on the in-plane behavior of unreinforced masonry (URM) infill walls installed in reinforced concrete (RC) frames based on the experimental study. Five 1/2-scale specimens of single span, single story RC frames with masonry infill walls were tested using a static cyclic loading protocol. In the present study, the seismic capacity in terms of strength, stiffness and deformation were studied based on the influence of three main parameters:

- 1- Varying the strength of surrounding RC columns.
- 2- Varying the strength of RC beam.
- 3- Varying strength of mortar used in the masonry infill.

2. EXPERIMENTAL PROGRAM

2.1 Test specimens

As stated previously, five half-scaled specimens were designed based on three main parameters: i) varying ratio of RC column strength to masonry infill lateral strength, ii) varying the strength and stiffness of RC beam (very rigid strong beam and relatively flexible beam), iii) varying the strength of masonry's mortar. The design concept of specimen for each parameters is explained as follows:

2.1.1 Specimen of Series i) varying ratio of RC column strength to masonry infill lateral strength.

The parameter of the relative strength of the boundary RC frame to the masonry infill is a crucial parameter that not only governs the behavior and failure modes of the RC frame but also the strength and failure mode of the masonry infill. This was demonstrated in an experimental study conducted by Mehrabi et al (1996). A study by Wood (1978) emphasized the impact of frame to masonry infill strength ratio on failure mechanism and proposed empirical equations to calculate shear strength based on this ratio. However, other codes such as ASCE/SEI 41 (2006) proposed equations to calculate the masonry infill strength based on shear tests of masonry infill ignoring the frame to masonry infill strength ratio. In the ASCE/SEI 41 (2006), the strength ratio was used to determine deformation limits for the masonry infill. In addition, Flangan et al. (1999) based on his experimental study has concluded that the strength of compression failure mechanism of the masonry infill was not significantly influenced by the frame to masonry infill strength or stiffness ratios and instead proposed simplified empirical equations which did not use this parameter. In summary, the experimental results and equations proposed by various researchers tend to contradict each other. Some studies placed emphasis on the importance of the frame to infill strength ratio while other studies ignored it. Therefore, in this study, three half-scaled specimens with RC frames of different strength and having the same unreinforced masonry infills were designed to clarify the influence of this parameter. The parameter for test specimens of series *i*) is defined as the ratio of the boundary frame to masonry infill lateral strength named as β index, as shown in Equation 1.

$$\beta = V_f / V_{inf} \quad (1)$$

Where V_f is the boundary frame lateral strength which is calculated to be the ultimate flexural capacity of a bare frame with plastic hinges at top and bottom of columns. The V_{inf} is the masonry infill lateral strength calculated based on Equation 2 which is a simplified empirical equation showing good agreement with experimental database studied by the author (Al-Washali et al. 2017)

$$V_{inf} = 0.05 f_m \cdot t_{inf} \cdot l_{inf} \quad (2)$$

Where f_m is the compressive strength of masonry prism, t_{inf} is the infill thickness and l_{inf} is the infill length.

The frame to masonry infill lateral strength ratio in typical existing RC low-rise buildings of 4 stories in Bangladesh mentioned in the reference CNCRP (2015) are investigated. The case study of buildings in Bangladesh is considered since this experimental study is a part of a wider scope ongoing experimental

program of a Japanese project called SATREPS intended to upgrade seismic evaluation methods reinforced concrete buildings in Bangladesh. The β index for three investigated existing buildings varies between 0.3~0.8 for the outer frame where masonry wall thickness is typically 250mm. On the other hand, the β index for inner frames ranges between 0.5~1.5, since the infill thickness in inner-partitions is 125 mm, which is the half of that in the outer frame.

Based on these observations, three half-scaled specimens with different RC frames, having same unreinforced masonry infills, are designed representing lower, average and upper boundary of β index. Specimens are named F-0.4, F-0.6 and F-1.5 which represents the ratio of strength of frame to masonry, β index, of 0.4, 0.6 and 1.5, respectively. The beams were designed to be stronger and stiff enough to simulate a typical case of a weak column and strong beam system observed in existing old designed buildings. Thus, the frame lateral strength, V_f , of series i) depends mainly on the ultimate flexural capacity of plastic hinges at top and bottom of columns.

In previous research by Liauw et al. (1985) and Wood (1978), they emphasized how the masonry infill force changes the position of plastic hinges formed in RC frames during an in-plane lateral loading. The conventional assumption of plastic hinges formed at the top and bottom of the columns, can be altered in which lower hinge is formed in the middle or in the upper third region of the column. This cause a failure mechanism similar to a short column effect causing shear failure of a column with insufficient transverse reinforcement. In this research, to allow the full investigation of flexural behavior of the frame and plastic hinge positions, the columns are designed with additional transverse reinforcement to avoid shear failure in the case that plastic hinges might be formed at the middle of column. The specimen dimensions and details of series i) are shown in Figure 1. All 3 specimens were identical except for the column size and reinforcement, as shown in Figure 1.

2.1.2 Specimen of Series ii) varying strength and stiffness of beam

In the previously mentioned specimens of *series i)*, the beams were designed to be stronger and stiff enough to simulate a typical case of a weak column and strong beam system observed in existing buildings of old designs. However, the recent building codes of many countries emphasize to design buildings with strong column and weak beam, in order to increase the deformation capacity of a building and avoid story collapse mechanism of a building. Thus, in this study, one specimen (named as WB, weak beam) was designed with weak beam and strong column, in order to study the influence of this parameter on the seismic capacity and collapse mechanism of infilled RC frames. Specimen WB is designed to be exactly identical to specimen F-0.6 except for the upper beam which was relatively smaller and designed to have a ratio of beam plastic moment capacity, M_{ub} , to the column plastic moment capacity M_{uc} , of 0.7 ($M_{ub}/M_{uc} = 0.7$). The specimen dimensions and details of specimen WB are shown in Figure 2.

2.1.3 Specimen of Series iii) varying mortar strength of masonry infill wall

In the previously mentioned specimens of *series i)*, the mortar of infill walls was of very good quality with compressive strength of about 25 MPa. However, the masonry infill walls in many countries are considered as non-structural walls and thus low quality mortar strength is commonly used. Lowering mortar compressive strength will reduce prism compressive strength of masonry f_m . This will also reduce the shear strength of masonry infill as indicated in Equation 2.

On the other hand, compressive masonry prism material tests conducted by H. Kaushik et al. (2007) showed that masonry prism with low mortar strength has much greater strain at point of maximum compressive load which indicates greater deformation capacity. The most well recognized method for modeling masonry infill as macro models is using the equivalent diagonal compression strut which is recommended by many codes such as FEMA 306 (1998). Assuming that masonry infill acts as an ideal compressive strut, then lowering strength of mortar will increase deformation capacity assuming that it behaves as compressive material results of masonry prism tests. Thus, in this study, one specimen (named as WM, weak mortar) was constructed using very weak mortar in order to study the influence of this parameter on the seismic capacity and collapse mechanism of infilled RC frames. Specimen WM is designed to be exactly identical to specimen F-0.6 except for mortar strength. Summary of all 3 parameters and main differences between specimens is summarized in Table 1.

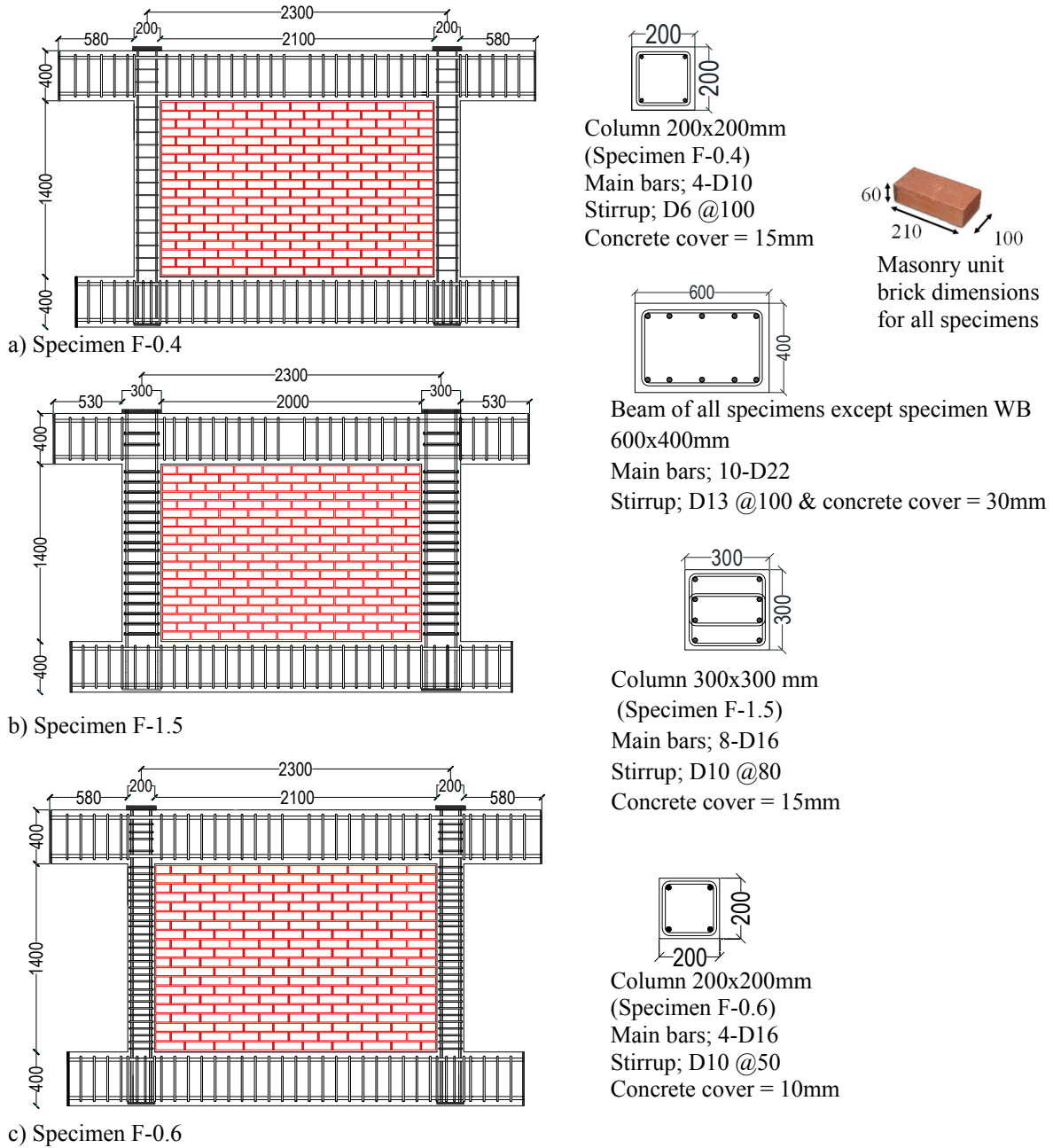


Figure 1. Dimensions and reinforcement of specimens of series *i* ; units in mm

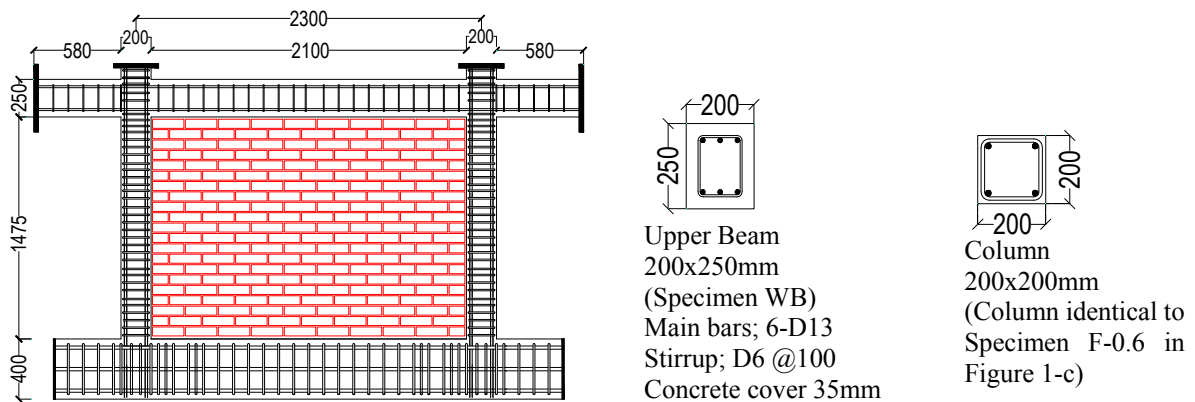


Figure 2. Dimensions and reinforcement of specimen WB (weak beam) ; units in mm

Table 1. Summary of specimen details and varying parameters

Series no.	Main varying parameter	Specimen name	β index	Column dimension (mm)	Beam dimension ($b \times d$) (mm)	Ratio M_{ub}/M_{uc} *	Mortar strength
<i>i</i>	Strength of RC column	F-1.5	1.51	300 x 300	600 x 400	3.3	Strong
		F-0.6	0.56	200 x 200		9.7	Strong
		F-0.4	0.39			5.9	Strong
<i>ii</i>	Weak beam	WB	0.43		200 x 250	0.7	Strong
<i>iii</i>	Weak mortar	WM	0.82		600 x 400	5.9	Weak

*ratio of beam to column's plastic moment capacity

2.2 Material properties

The infill panels are constructed using 60 x 100 x 210 mm solid bricks conventionally used in Japan. A professional mason built the infill, after the frame construction, where its thickness is 100mm and mortar head and bed joint thickness is about 10mm. Table 2 and Table 3 show the properties based on material tests conducted on the reinforcing steel, concrete and masonry respectively, where those values represent the mean values of three samples in each test. These include steel tensile strength by JIS Z 2201 (2010), the compression strength of concrete and mortar cylinders by JIS A 1108 (2010), the splitting tensile strength of concrete and mortar cylinders by JIS A 1113 (2010), the masonry prism compressive strength tested according to ASTM C1314 (2011). The concrete used for all specimens had the same mix design. The proportion of cement and sand for the mortar is 1:2.5 (mass proportion) for all specimens except for specimen WM with weak mortar where 1:6 is used. The masonry prism samples were made simultaneously with the infill panel by the same professional mason. The material tests were conducted at the same time with the experimental loading for each specimen individually. There are slight differences of compressive strength of concrete, mortar and masonry prism strength which is considered to be caused by the time gap between testing of specimens

Table 2. Material properties of Concrete and Masonry

Specimen name	Frame Concrete			Masonry Prism			Mortar cylinders	Brick unit Compressive strength (MPa)
	Compressive strength (MPa)	Elastic moduli (MPa)	Split Tensile strength (MPa)	Compressive strength (MPa)	Elastic moduli (MPa)	Strain at peak stress	Compressive strength (MPa)	
F-1.5	28.3	2.3×10^4	2.4	18.6	8140	0.0039	29.2	38.1
F-0.6	25.5	2.4×10^4	2	19.5	10230	0.0036	27.7	
F-0.4	24.2	2.3×10^4	2.1	17.3	7840	0.0037	20.2	
WB	23.6	2.4×10^4	1.9	19.5	10230	0.0036	27.7	
WM	25.8	2.3×10^4	2	13.3	5470	0.0059	4.8	

Table 3 Reinforcement mechanical properties

Bar	Nominal strength	Yield strength (MPa)	Ultimate tensile strength (MPa)
D6	SD345	346	546
D10	SD345	384	576
D13	SD345	380	568
D16	SD345	380	563
D22	SD390	447	619

2.3 Test setup and instrumentation

The loading system is shown schematically in Figure 3 and Figure 4. The vertical load was applied on RC columns by two vertical hydraulic jacks and was maintained to be 200kN on each column. Two pantograph, attached with the vertical jacks, restricted any torsional and out-of-plane displacement. Two horizontal jacks, applying together an incremental cyclic loading, were attached at the beam level and were controlled by a drift angle of $R\%$, defined as the ratio of lateral story deformation to the story height measured at the middle depth of the beam ($h=1,600\text{mm}$). The lateral loading program consisted of 2 cycles for each peak drift angle of 0.05%, 0.1%, 0.2%, 0.4%, 0.6%, 0.8%, 1%, 1.5% and 2 %. Specimens, which didn't significantly degrade in strength after the 2nd cycle of 2 %, were then pushed monotonically until severe damage or significant degradation of strength is observed. Locations of LVDTs are schematically shown in Figure 5. The story drift is measured using LVDTs attached on the middle height of beam. In addition, strain gauges were attached on main reinforcing bars of columns and beams at critical sections and distributed uniformly at every 200 mm.

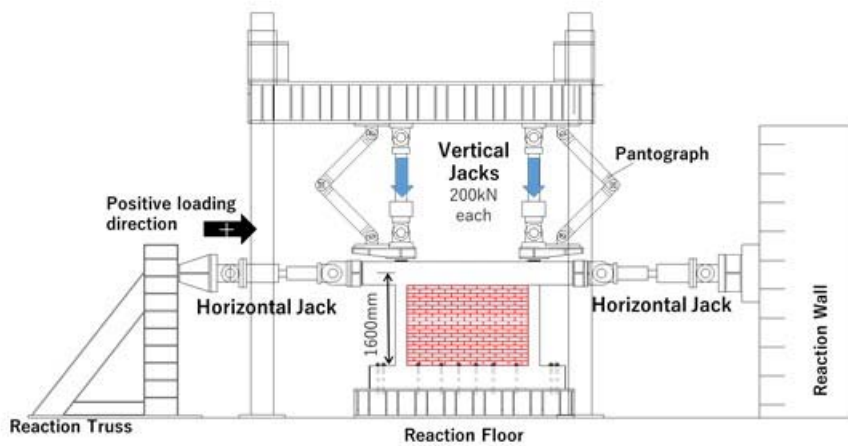


Figure 3. Test setup (units: mm)



Figure 4. Test setup (units: mm)

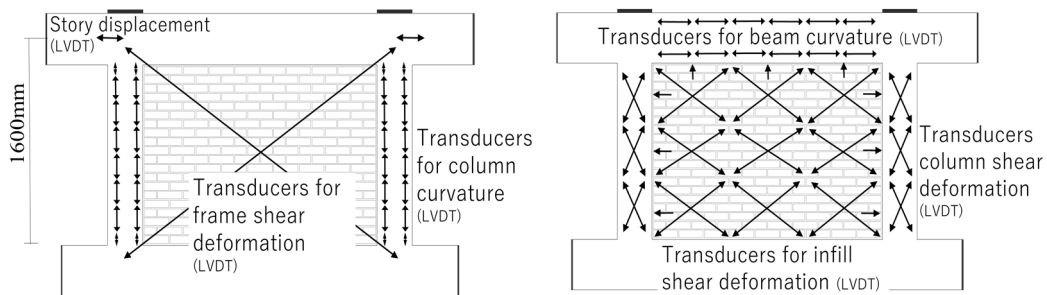


Figure 5. Schematic figure of Instrumentation details

3. EXPERIMENTAL RESULTS:

The lateral load versus story drift angle graphs of all specimens are shown in Figure 6. Cracks and failure patterns after final drift cycle of 2.0% are shown in Figure 7.

For Specimen F-0.4:

Very small and few cracks on mortar bed joint and diagonal cracks on bricks near loading corner of infill panel, less than 0.3mm width, started at early stages of loading just when the drift angle was 0.05%. At drift angles of 0.2% and 0.4%, the longitudinal reinforcement in the tensile column (windward column) yielded at the upper critical section and just above its mid-height, respectively, forming failure mechanism similar to a short column. Just after reaching the maximum lateral strength at story drift of 0.8%, there was a sudden drop of lateral load bearing capacity with extensive cracking and spalling of bricks. After the drift of 1%, the main failure mechanism changed from diagonal cracks to sliding cracks with clear sliding movement at the mid-height of the infill. At drift story of 2% in the negative cycle, the concrete around the reinforcement of top compression column spalled-off and main bars buckled.

For Specimen F-0.6:

Very small cracks on mortar bed joint and diagonal cracks on bricks near loading corner of infill panel, less than 0.05mm width, started at early stages of loading just when the drift angle was 0.05%. At drift angles of 0.1%, cracks became more visible on masonry infill wall with max crack width of 0.5mm. At drift angle between 0.6%~0.8%, the longitudinal reinforcement in the tensile column (windward column) yielded at the upper critical section and above its mid-height, respectively, forming failure mechanism similar to a short column, which is similar to behavior observed in specimen F-0.4. The compression column (lee-ward column) yielded as top and bottom of column height (similar to behavior of bare frame). The shear cracks concentrated at the upper third part of columns as shown in figure 6 and stirrups yielded at drift angle of 0.8%. The damage of masonry infill was also concentrated at the top corners with almost no damage at mid span. The main variance with the specimen F-0.4 is that strength deterioration was not of a sudden after reaching the maximum lateral strength. After the drift of 2%, the shear cracks in the upper region of columns extended and concrete cover spalled off and main reinforcement became visible. However, the columns continued to carry load and did not buckle even after story drift angle of 3%.

For Specimen F-1.5:

Cracking of infill panel also started at the peak of the first loading cycle, which was relatively similar to the crack width observed in specimen F-0.4 at this stage. At drift angle between 0.6%~0.7%, both columns yielded at the locations of bottom and top sections (similar to behavior of bare frame). As it reached its maximum strength, the lateral load gradually degraded (contrarily to the sudden degradation of strength in previous specimen F-0.4) with the drift angle increase until 1.5%, where there was a slight drop of the lateral load, after the horizontal sliding between bricks clearly increased. At the drift angle of 2%, the loading stopped as planned, and the masonry infill damage at this point was much greater than observed in the previous specimen F-0.4 (see Figure 7). In spite that columns had many cracks, there was no extensive damage or spalling of concrete cover.

For Specimen WB (weak beam):

Contrary to previous specimen F-0.6 with strong beam, relatively more cracks occurred at the beam and infill panel at story drift of 0.05% with width of about 0.2 mm in infill and 0.05 mm in beam. There was a slight and sudden drop of strength at drift angle 0.1%, but strength started to increase again until it reached max strength at story drift of 0.8%. At drift angle 0.6%, longitudinal reinforcement in upper beam yielded at both edges near the joint. At drift of 0.8%, the tensile column (windward column) yielded at about mid-height forming a short column mechanism similar to specimen F-0.6, the compression column (leeward column) formed hinge at lower critical section with stub. The damage of infill panel was concentrated at upper half and near loading corners, with almost no damage middle lower part of infill panel. The main variation with specimen F-0.6 (identical specimen but with strong beam) was that strength degraded at a faster rate. At drift story of 2%, cracks in beam and columns opened greatly with maximum crack width of about 3 mm, but there were no spalling of concrete cover.

For Specimen WM (weak mortar):

Contrary to previous specimen F-0.6 with stronger mortar and identical RC frame, cracks didn't occur at story drift of 0.05% in specimen WM. Very small cracks at mortar bed joint and diagonal on bricks started to be noticed from 0.1%. At drift angle between 0.6%~0.8%, both columns yielded at the locations bottom and top sections (similar to locations of hinges of specimen F-1.5). The lateral load slightly degraded in the positive loading after 1%. However, there was no significant degradation of strength in the negative loading and maximum strength reached at drift of 1.5 %. Even though the mortar strength and masonry strength are much weaker as shown in previously in Table 2, the maximum lateral strength were almost similar to specimen F-0.6. The main variation from specimen F-0.6 was that surrounding RC columns avoided forming hinge in the middle of height of column and had relatively much less damage. Comparison of damage level and cracks at drift angle of 2% showed that the damage on masonry infill and RC columns was relatively much less than other specimens with no signs of shear failure or spalling of masonry or concrete cover, as shown in Figure 7.

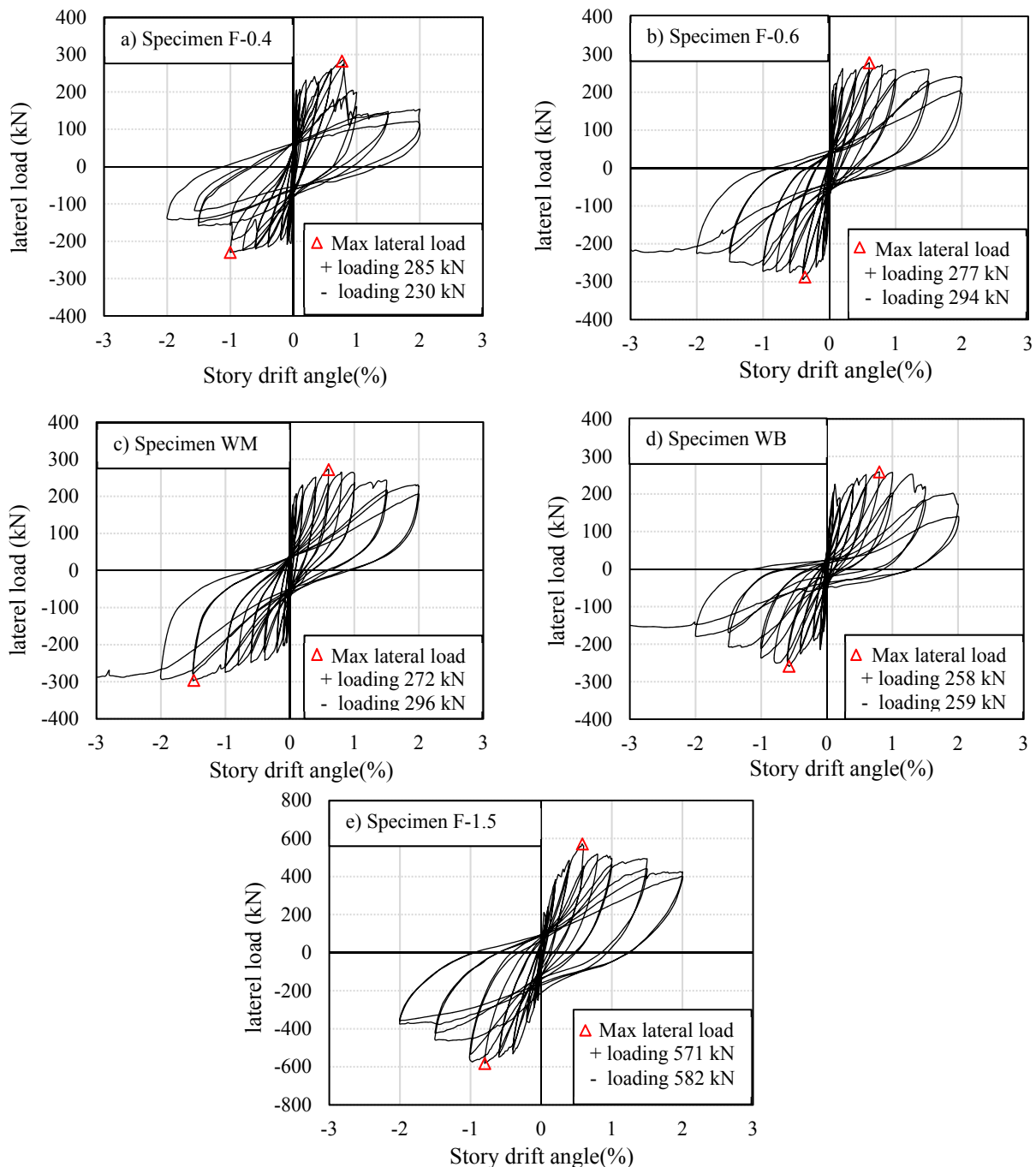
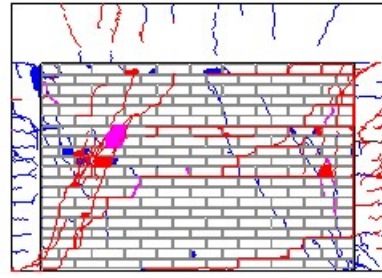
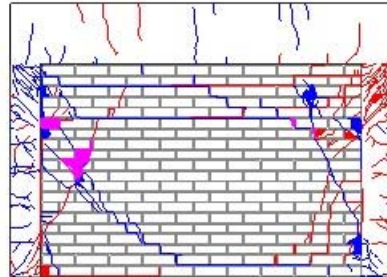


Figure 6. Lateral strength & story drift angle for all specimens : a)-e)

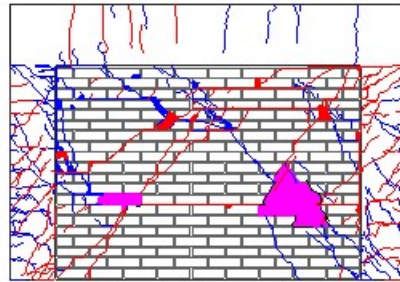
a) Specimen F-0.4



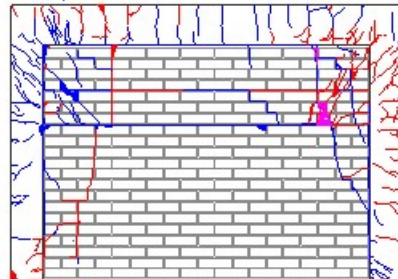
b) Specimen F-0.6



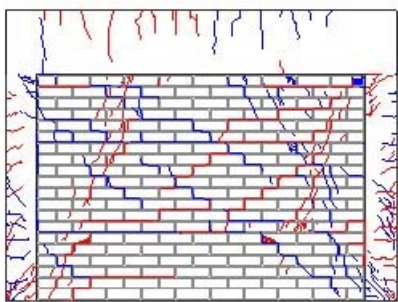
c) Specimen F-1.5



d) Specimen WB



e) Specimen WM



— Cracks during + loading

■ Spalling of cover during + loading

■ Holes on masonry infill (can see through)

— Cracks during - loading

■ Spalling of cover during - loading

Figure 7. Crack patterns observed at story drift of 2% for all specimens : a)~e)

4. DISSCUSSION OF EXPERIMENTAL RESULTS:

4.1 Strength

The maximum lateral load contributed by the masonry infill (V_{inf}) is calculated by deducting the bare frame lateral strength (V_f) from the maximum lateral load of the overall structure (V_{max}), as shown in Equation (3). Actual maximum lateral strength of the structure can be more complicated than summation of the shear strength of bare frame and masonry infill, due to the complicated frame-panel interaction, variation of hinge locations and internal varying axial load on columns; therefore, in this study, Equation (3) is employed as comparison benchmark.

$$V_{inf} = V_{max} - V_f \quad (3)$$

$$V_f = 4Mu/h_o \quad (4)$$

Where M_u is the minimum plastic moment of the column or beam calculated by AIJ provision (2016) and h_o is the clear height of column (taken here as infill height). The moment capacity of columns ends where calculated using axial load applied by vertical jacks of 200kN.

Table 4 shows the experimental shear strength of masonry infills τ_{inf} in all specimens, which is the shear force (V_{inf}) divided by the infill cross-sectional area.

Table 4 Shear strength of masonry infill

No.	Experiment V_{max} (kN)		V_f (kN) Eq(3)	Experiment V_{inf} (kN) by Eq(4)		Maximum shear strength τ_{inf} (N/mm ²)		Average V_{inf} of both directions (kN)	Avg. shear strength τ_{inf} both directions (N/mm ²)
	Positive loading	Negative loading		Positive loading	Negative loading	Positive loading	Negative loading		
F-0.4	285	230	71	214	159	1.07	0.75	186.5	0.88
F-0.6	277	295	113	164	182	0.78	0.87	173	0.82
F-1.5	571	582	280	291	302	1.46	1.51	296.5	1.48
WB	258	259	88	170	171	0.81	0.81	170.5	0.81
WM	272	296	113	159	183	0.76	0.87	171	0.81

The shear strength of all specimens, except for F-1.5, are of the same range between 0.8~0.9 MPa. Specimen F-1.5 has the shear capacity of 1.48 N/mm² which is about 1.5 times other specimens. Figure 8 shows the relation of masonry infill shear strength, τ_{inf} (normalized by prism compressive strength f_m), with parameter β index (ratio of the boundary frame to masonry infill lateral strength). As shown in Figure 8, there is a clear relation between the increase of β index and increase of shear strength. The large increase in shear strength is thought to be mainly due to confinement effect of the stronger boundary frame. It is thought that the stronger and stiffer the boundary RC frame will result in increase in the contact length between frame and masonry infill. Thus, increases of the infill's compression strut width increase the lateral strength capacity. Interestingly, there was no significant decrease of shear strength for masonry infill with weak mortar, and it is thought that weaker masonry infill had wider strut width, allowing infill panel to carry more lateral load.

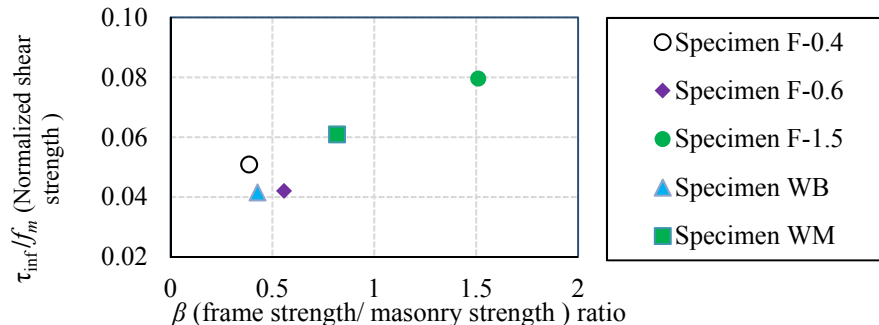


Figure 8. Relation between β index and shear strength of infill normalized by prism compressive strength

4.2 Initial stiffness

The initial stiffness of infilled frame is taken as the slope between the origin point of the load-displacement curve and the point at which there is a major visible crack in the masonry infill and the RC frame, which was

determined to occur at story drift of 0.1% as shown in Figure 9. From this results, it is concluded that the investigated parameters did not significantly influence the initial stiffness.

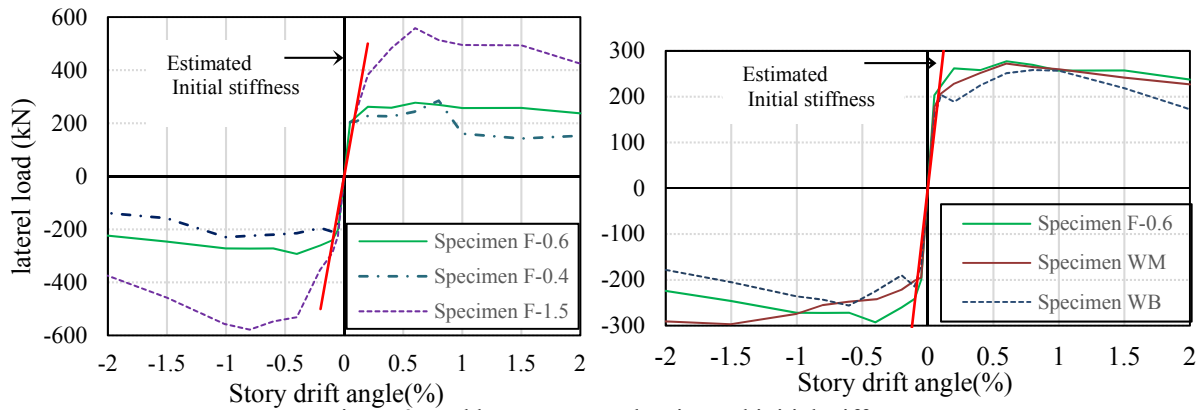


Figure 9. Backbone curve and estimated initial stiffness.

The most well recognized method for calculating the infill stiffness is using the equivalent diagonal compression strut, which has the same elasticity and thickness as the infill panel. Many researchers and codes such as FEMA 306 (1998) have suggested equations to estimate the equivalent strut width (W_{ef}). However, there are large variations in strut width assumptions between different codes. The equivalent strut width is calculated from the experiment results using the masonry infill elasticity previous mentioned in Table 1 and initial stiffness shown in Figure 9. The equivalent strut width (W_{ef}) is normalized by diagonal length of infill panel (d_m) and shown Figure 10. Based in the results of this study, the W_{ef} ranges between $0.15d_m \sim 0.29d_m$ with an average of $0.2d_m$. Paulay et al. (1992) recommended using the effective width of strut (W_{ef}) as $0.25d_m$, but this study shows that Paulay et al's simplified equations might slightly overestimate the initial stiffness. On the other hand, both FEMA 306 (1998) and ASCE/SEI 41 (2006) recommend the Mainstone's empirical equation which in this study gave strut width of $0.1d_m$ for all specimens except specimen F-1.5 it was of $0.12d_m$ which greatly underestimated the initial stiffness.

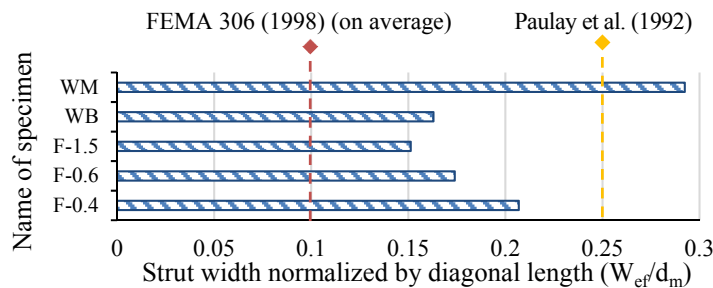


Figure 10. Effective width of strut based on estimated initial stiffness

4.3 Ductility

In this study, R_{crack} , R_{max} and R_u are the representative drift angles at the cracking, the maximum strength and the strength degradation point, respectively. Strength degradation point R_u is set to be 80% of the maximum strength. It should be noted that R_u does not indicate the safety deformation limit, but used herein for comparison benchmark. The R_{crack} , R_{max} and R_u are estimated using the backbone curves in Figure 9 previously shown. Normalized envelop for positive loading is shown in Figure 11.

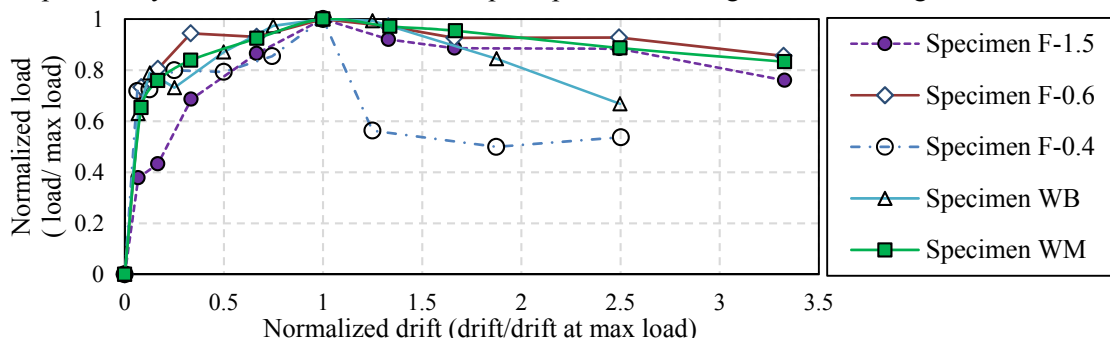


Figure 11. Normalized envelopes (load/max load vs. drift/drift at max load)

R_{-crack} is estimated to be 0.1%~0.2% for all specimens which small cracking became clearly visible which could be assumed as immediate occupancy level. The R_{-max} (drift at peak strength), of all specimens is estimated to be around 0.8%, except for specimen WM with weak mortar in the negative cycle which was found to be 1.5%. This indicates that weak mortar had greater deformation capacity. For R_u , Specimen F-0.4 (with very weak column relative to masonry infill), there was a sudden drop of strength at story drift of about 0.9%. R_u of specimen F-0.6, F-1.5 and WB had was about 1.5%. The R_u could be taken as ultimate safety level (ULS). Based on the results in this study, the parameter of varying the surrounding frame strength had slight influence on R_{-crack} and R_{-max} , but greatly influenced the strength degradation slope and R_u . Specimen WM (weak mortar) showed the beneficial influence of weak mortar, as there was almost no degradation of strength and relatively less damage in masonry infill panel and surrounding frame. However, the influence of weak mortar might have adverse effects on out of plane capacity that need further study.

5. CONCLUSIONS

This paper presents the results of an experimental study of five specimens of masonry infilled RC frames and the followings are major findings:

- a) Experimental results showed that as the ratio of frame shear strength to masonry shear strength increased, there was great improvement of the masonry infill walls in terms of strength and avoidance of sudden brittle behavior of the masonry infill.
- b) The post-peak degradation slope was also improved with increasing the ratio of frame shear strength to masonry infill. This parameter should be taken into account in the design code of new RC buildings with masonry infill as it can change the brittle behaviour to relatively ductile behaviour.
- c) Interestingly, specimen WM (weak mortar) showed beneficial influence of weak mortar, as there was relatively less damage in masonry infill panel and surrounding frame. However, the influence of weak mortar might have adverse effects on out of plane capacity, which is out of scope of this study.

6. ACKNOWLEDGMENTS

This study was sponsored by the (SATREPS) project funded by JST (Japan Science and Technology Agency) and JICA (Japan International Cooperation Agency) for Bangladesh, 2015 project headed by Professor Nakano Yoshiaki, University of Tokyo and it's gratefully acknowledged.

7. REFERENCES

- Al-Washali H, Suzuki Y, Maeda M (2017) Seismic evaluation of reinforced concrete buildings with masonry infill wall. In: *The 16th world conference of earthquake engineering, Chile*.
- American Society of Civil Engineers (ASCE) (2007) *Seismic rehabilitation of existing buildings*. Reston, Virginia (ASCE/SEI 41-06)
- American Society of Testing and Materials (ASTM) (2011) *Standard test method for compressive strength of masonry prisms*. ASTM C1314, West Conshohocken, PA
- Architectural Institute of Japan (AIJ) (2016) *AIJ standard for lateral load-carrying capacity calculation of reinforced concrete structures* (in Japanese)
- FEMA 306 (1998) Evaluation of earthquake damaged concrete and masonry wall buildings, *Applied Technology Council (ATC-43 Project)*
- Flanagan RD, Bennett RM (1999) In-plane behavior of structural clay tile infilled frames. *J Struct Eng* 125(6).
- Japanese Industrial Standards (2010), No. *JIS R1250, JIS Z 2201, JIS A 1108, JIS A 1113 Japanese Standards Association* (in Japanese)
- Kaushik HB, Rai DC, Jain SK (2007) Stress-strain characteristics of clay brick masonry under uniaxial compression. *J Mater Civil Eng (ASCE)* 19(9):728–739
- Liauw TC, Kwan KH (1985) Unified Plastic analysis for infilled frames. *J Struct Eng* 111(7):1427–1448
- Mehrabi AB, Shing PB, Schuller M, Noland J (1996) Experimental evaluation of masonry-infilled RC frames. *J Struct Eng ASCE* 122(3):228–237
- Paulay, T. and Priestley, M.J.N. (1992) *Seismic design of reinforced concrete and masonry buildings*. Wiley, NY
- Project for Capacity Development and Retrofitting for Public Buildings, (2015). Public Works Department, Bangladesh. *Manual for Seismic Evaluation of Existing Reinforced Concrete Building*.
- Turgay T, Durmus MC, Binici B, Ozcebe G (2014) Evaluation of the predictive models for stiffness, strength, and deformation capacity of RC frames with masonry infill walls. *J Struct Eng* 140:06014003. doi:10.1061/(ASCE)ST.1943-541X.0001069
- Wood RH (1978) Plasticity, composite action and collapse design of unreinforced shear wall panels in frames. *Proc Inst Civil Eng Part 2* 65:381–411